International Journal of Electrical and Computer Engineering (IJECE)
Vol. 7, No. 2, April 2017, pp. 667~680
ISSN: 2088-8708, DOI: 10.11591/ijece.v7i2.pp667-680

Voltage Compensation in Wind Power System using STATCOM Controlled by Soft Computing Techniques

Bineeta Mukhopadhyay, Rajib Kumar Mandal, Girish Kumar Choudhary
Department of Electrical Engineering, National Institute of Technology, Patna, India

Article Info

Article history:

Received Aug 26, 2016
Revised Feb 24, 2017
Accepted Mar 8, 2017

Keyword:

Doubly fed induction generator (DFIG)
Fuzzy logic
Particle swarm optimization (PSO)
Point of common coupling (PCC)
Static synchronous compensator (STATCOM)

ABSTRACT

When severe voltage sags occur in weak power systemsassociated with grid-connected wind farms employing doubly fed induction generators, voltage instability occurs, which may lead to forced disconnection of wind turbine. Shunt flexible AC transmission system devices like static synchronous compensator (STATCOM) may be harnessed to provide voltage support by dynamic injection of reactive power.In this work, the STATCOM provided voltage compensation at the point of common coupling in five test cases, namely, simultaneous occurrence of step change (drop) in wind speed and dip in grid voltage, single line to ground, line to line, double line to ground faults and sudden increment in load by more than a thousand times. Three techniques were employed to control the STATCOM, namely, fuzzy logic, particle swarm optimization and a combination of both. A performance comparison was made among the three soft computing techniques used to control the STATCOM on the basis of the amount of voltage compensation offered at the point of common coupling. The simulations were done with the help of SimPowerSystems available with MATLAB / SIMULINK and the results validated that the STATCOM controlled by all the three techniques offered voltage compensation in all the cases considered.

Corresponding Author:

Bineeta Mukhopadhyay,
Department of Electrical Engineering,
National Institute of Technology, Patna, India.
Email: bineeta2010@gmail.com

1. INTRODUCTION

Considering that the total global wind power production at the end of 2015 was 432883 MW (data provided by the official website of Global Wind Energy Council), wind is definitely one of the key renewable power sources which are transforming the power sector. The suitability of DFIG for grid-connected wind power generation has been illustrated by enumerating its benefits including superior voltage control and compensation of reactive power, supply of good quality controllable power at low wind speeds, decoupled control of real and reactive power and extraction of maximum power and its ability to ride throughvoltage dips and faults [1], [2]. Fluctuations in voltage, harmonics, inadequate reactive power support and poor power factor are some common issues which occur in grid-linked wind energy systems, leading to unsatisfactory performance of devices, unwanted tripping of protection elements and damage to sensitive apparatus. Voltage dip due to low wind speeds, disturbances in the grid, faults and unexpected load variations is one of the most serious issues occurring in grid-connected wind power systems [3]. When faults or disturbances occur in the system, the rotor of the DFIG is short-circuited and the rotor side converter is blocked so that the rotor does not get damaged due to overcurrents. Although the wind farm supplies reduced power in case of faults, it remains in service. However, if severe voltage dips occur in a weak power system (with a low short-circuit ratio and often subjected to low voltage conditions) connected to DFIG-based wind farm, the DFIG grid side converter which has a low rating is unable to provide the required voltage and reactive power support. Consequently, the system may be subjected to voltage instability. In such cases, it

becomes compulsory to disconnect the wind turbines and later connect them again after the clearance of the fault. This makes the system highly unreliable. The international grid codes are very strict when it comes to low-voltage ride through and make it compulsory to ensure that the wind farms do not become unstable and get disconnected even when the voltage dips to a very low value.

This voltage instability issue can be resolved by employing flexible AC transmission system (FACTS) compensators like static synchronous compensators (STATCOM), which provide transient and steady-state voltage support at the point of common coupling (PCC) by means of dynamic reactive power injection. In spite of the huge expenses involved, the STATCOM is preferred over some other FACTS devices due to its superior performance and flexibility. The reactive power support offered by the STATCOM at lower voltages is greater than that offered by SVC. Also, the response of SVC is slow compared to STATCOM due to firing delays associated with SVC. Research attempts have been directed towards the real time utilization of STATCOM to maintain voltage stability in a weak power system connected to DFIG-based wind farm [4], [5]. The role of FACTS devices in enhancing the stability of grid-connected wind power systems has been enumerated in detail [6]. Fuzzy logic and ANFIS-based control for the STATCOM in a grid-connected PMSG-based wind power system was proposed [7]. AnLuo,et al suggested a fuzzy-PI independent control technique for STATCOM in distribution networks [8]. Fuzzy logic may be memory-intensive and may lead to software overload, particularly in less complicated applications, owing to the use of many localized parameters. Particle swarm optimization (PSO) is acomputationally efficient swarm intelligence based optimization technique which involves cognitive and social interactions and has often demonstrated fast response and improved performance compared to fuzzy controllers. Previously, research work has been done in the field of PSO-controlled STATCOM and in the area of DFIG-based wind farms separately. However, this is a novel attempt to integrate PSO-controlled STATCOM in DFIG-based grid-connected wind power systems. Chien-Hung Liu, et al proposed a flexible controller for STATCOM using PSO, using integral absolute error (IAE) as the evaluation criterion [9]. However, although minimization problems employing IAE as the objective function produce a low overshoot response, they suffer from the drawback of excessively long settling times. Therefore, in this work, a different evaluation criterion was used in the PSO program used to control the STATCOM.

In this work, STATCOM wasemployed for providing voltage compensation at the PCC in a DFIG-based grid-connected wind power system in five test cases, namely, step change (drop) in wind speed simultaneously accompanied by a dip in grid voltage, single line to ground (SLG), line to line (LL), double line to ground (DLG) faults and sudden load increment. The STATCOM was controlled using three soft computing techniques, namely, fuzzy logic (research method 1), PSO (research method 2) and a combination of both fuzzy logic and PSO (research method 3). In the third methodology, both fuzzy logic and PSO were used to tune the PI controller gains in the STATCOM voltage supervisor. This methodology, called fuzzy PSO-PI technique, is a novel STATCOM control technique. Also, it has been used in wind power for the first time. A performance comparison was done among the three artificial intelligence based techniques used to control the STATCOM in terms of the amount of voltage compensation offered at the PCC in all the five test cases. The uniqueness of this research endeavour is also highlighted in two novel test cases which have been considered here, namely, occurrence of step change (drop) in wind speed and grid voltage dip at the same instant and abrupt variation in load by more than a thousand times.

2. MATHEMATICAL MODELLING OF WIND TURBINE AND DFIG

The net mechanical power obtained from a wind turbine $P_{extracted}$ is given by Equation (1):

$$P_{extracted} = 0.5\rho_a \pi R^2 V_{wind}^3 C_{w\_power} \quad (1)$$

In Equation (1), ρ_a, R, V_{wind} and C_{w_power} denote the air density, turbine blade radius, wind velocity and power coefficient of wind turbine respectively.

It is seen that: $C_{w\_power} = \frac{(1+\gamma)(1-\gamma^2)}{2}$ (2)

In Equation (2), γ is the tip speed ratio of the wind turbine which is given by: $\gamma = \frac{\text{blade tip speed}}{\text{speed of wind}}$

If γ = (1/3) in Equation (2), the value of power coefficient C_{w_power} is the maximum and the maximum value is equal to (16/27) = 0.59. This validates the Betz' principle which states that a maximum of 59.3% of the total kinetic energy possessed by wind is converted into mechanical energy [10]. The schematic representation of a wind energy conversion system employing DFIG is shown in Figure 1.

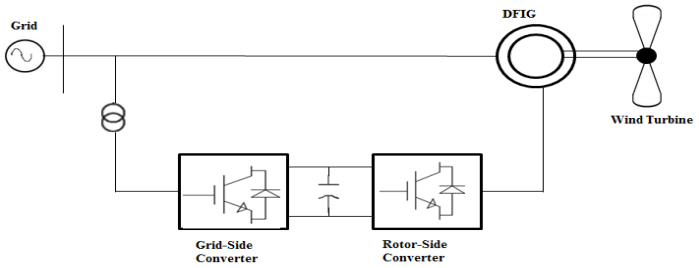

Figure 1. Schematic Diagram of DFIG-based wind power system

A variable frequency ac/dc/ac converter (VFC), which is supposed to control only 25% to 30% of the total power, links the rotor of the DFIG with the grid. The capacitor in the DC link between the Rotor-Side Converter (RSC) and the Grid-Side Converter (GSC) stores energy and reduces ripple in the DC link. The RSC reliably supervises the real and reactive power, speed, torque and power factor at the stator side. Supervision of the voltage of the DC link and provision of regulated reactive power support is done by the GSC.

The DFIG Equations in the dq reference frame for the stator voltages E_{sd} (d-axis) and $E_{s\ q}$(q-axis) and the rotor voltages E_{rd} (d-axis) and E_{rq} (q-axis) are stated in Equations (3)–(6) as follows [11]:

$$E_{sd} = R_s I_{sd} - \omega\lambda_{sq} + \frac{d\lambda_{sd}}{dt} \quad (3)$$

$$E_{sq} = R_s I_{sq} + \omega\lambda_{sd} + \frac{d\lambda_{sq}}{dt} \quad (4)$$

$$E_{rd} = R_r I_{rd} - (\omega - \omega_r)\lambda_{rq} + \frac{d\lambda_{rd}}{dt} \quad (5)$$

$$E_{rq} = R_r I_{rq} - (\omega - \omega_r)\lambda_{rd} + \frac{d\lambda_{rq}}{dt} \quad (6)$$

In Equations (3)-(6), I_{sd}, I_{sq}, I_{rd}, I_{rq}, $R_{s,}$ R_r, λ_{sd}, λ_{sq}, λ_{rd}, λ_{rq}, ω and ω_r represent d-axis stator current, q-axis stator current, d-axis rotor current, q-axis rotor current, per-phase stator resistance, per-phase rotor resistance, d-axis stator flux linkage, q-axis stator flux linkage, d-axis rotor flux linkage, q-axis rotor flux linkage, rotation speed of dq reference frame and electrical angular speed of the rotor respectively.The Equation relating the mechanical rotation speed of the DFIG $\omega_{mech}$and electrical angular speed $\omega_r$is given by$\omega_{mech} = \frac{2}{p}(\omega_r)$.

The expression for the electromagnetic torque developed $T_{developed}$ is given in Equation (7):

$$T_{developed} = \frac{3P}{4}(I_{sq}\lambda_{sd} - I_{sd}\lambda_{sq}) \quad (7)$$

The relationship between the mechanical rotation speed of the DFIG ω_{mech}, developed electromagnetic torque $T_{developed}$ and the mechanical torque applied T_{ex} is stated in Equation (8):

$$J\frac{d\omega_{mech}}{dt} = T_{ex} + T_{developed} \quad (8)$$

In Equation (8), J is the combined polar moment of inertia of the DFIG and prime mover with reference to the shaft of the machine.

3. STATCOM AND ITS CONTROL SYSTEM

In the STATCOM equivalent circuit in Figure 2, the converter losses are accounted for by $R_{dc,}$ V_{dc} is the voltage across DC capacitor C_{dc}, R_s and L_s denote the resistance and inductance of the coupling transformer respectively, V and Θ stand for the magnitude and phase angle of STATCOM RMS voltage respectively, u is the modulation ratio and the phase shift is β and the STATCOM currents in dq reference frame are I_d and I_q [12].

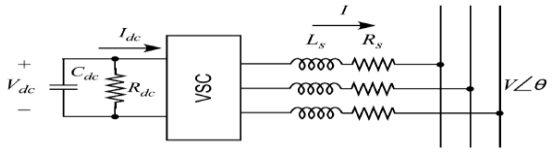

Figure 2. STATCOM Equivalent Circuit

In the dq reference frame, the state Equation of the STATCOM is given by Equation (9):

$$\frac{C_{dc}}{w_s}\frac{dV_{dc}}{dt} = -(I_d v_d + I_q v_q + \frac{V_{dc}}{R_{dc}}) \quad (9)$$

In Equation (9), $v_d = u\cos(\beta + \theta)$ and $v_q = u\sin(\beta + \theta)$

In the overall block schematic representation of the STATCOM control system is shown in Figure 3, the phase locked loop provides the angle φ for the computation of d-axis and q-axis components of voltages and currents in the STATCOM control system. The AC voltage controller and DC voltage controller generate the reference currents Ref_I_Q and Ref_I_D respectively. The current regulator operates on the error between the reference and actual q-axis (reactive) currents [13]. The frequency regulator acts on the difference between the standard grid frequency and the DFIG frequency and provided ΔRef_I_Q, which is added to Ref_I_Q generated by the voltage regulator to get the final value of reference reactive current Ref_I_Q (f).

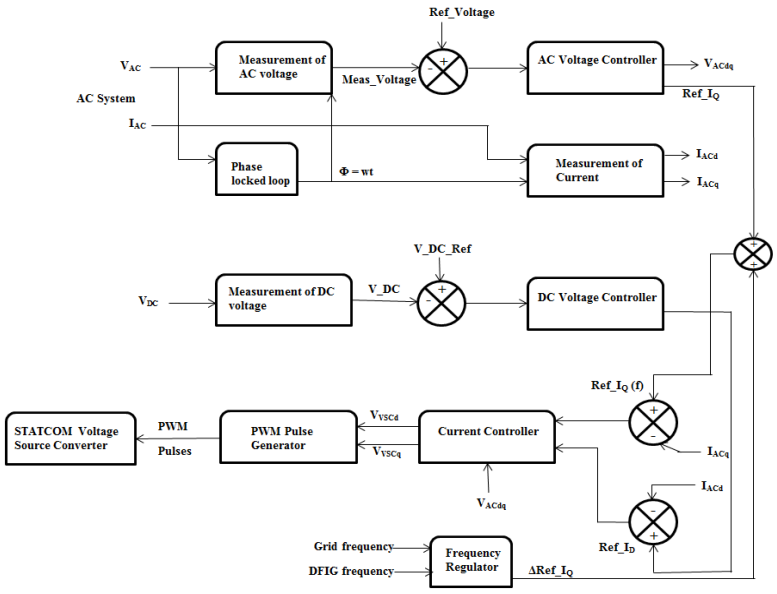

Figure 3. Overall Block Diagram of STATCOM Control System

4. RESEARCH METHOD 1: STATCOM CONTROLLED BY FUZZY LOGIC

The STATCOM performance was enhanced by including fuzzy logic controllers in the voltage, current and frequency regulator blocks of the STATCOM control system. Mamdani fuzzy inference technique was used and the fuzzy outputs were defuzzified using Centre of Area (COA) defuzzification. In the voltage and current regulators, fuzzy logic was used to tune the proportional and integral gain constants of PI controllers; hence this control methodology was termed fuzzy-PI technique. In the STATCOM current and voltage supervisors, the increments in the PI controller gains obtained from fuzzy logic controller, ΔK_{PR} (fuzzy) and ΔK_{IN} (fuzzy), were summed up with the original gain constants of the existing PI controllers, K_{PR} (PI) and K_{IN} (PI), to get the final tuned PI controller gains, K_{PR} (tuned) and K_{IN} (tuned), as shown in Equations (10) and (11):

$$K_{PR}\,(\text{tuned}) = K_{PR}\,(\text{PI}) + \Delta K_{PR}\,(\text{fuzzy}) \quad (10)$$

$$K_{IN}\,(\text{tuned}) = K_{IN}\,(\text{PI}) + \Delta K_{IN}\,(\text{fuzzy}) \quad (11)$$

The schematic diagram of the STATCOM voltage regulator supervised using fuzzy-PI technique is shown in Figure 4. In the fuzzy-PI regulated STATCOM voltage supervisor, the difference between the reference voltage (Ref_Voltage) and the measured (actual) value of voltage (Meas_Voltage), which is represented by v_{err}, and the first derivative of this deviation dv_{err}/dt were fed as inputs to the fuzzy system. The fuzzy controller provided the required changes in controller gains, ΔK_{PR} (fuzzy) and ΔK_{IN} (fuzzy). The new PI controller with modified proportional and integral gain constants, K_{PR} (tuned) and K_{IN} (tuned), was used to control the STATCOM voltage supervisor. The reference reactive current Ref_I_Q was provided by the STATCOM voltage regulator. The slope of the STATCOM V-I characteristics when it operates in voltage regulation mode is called droop.

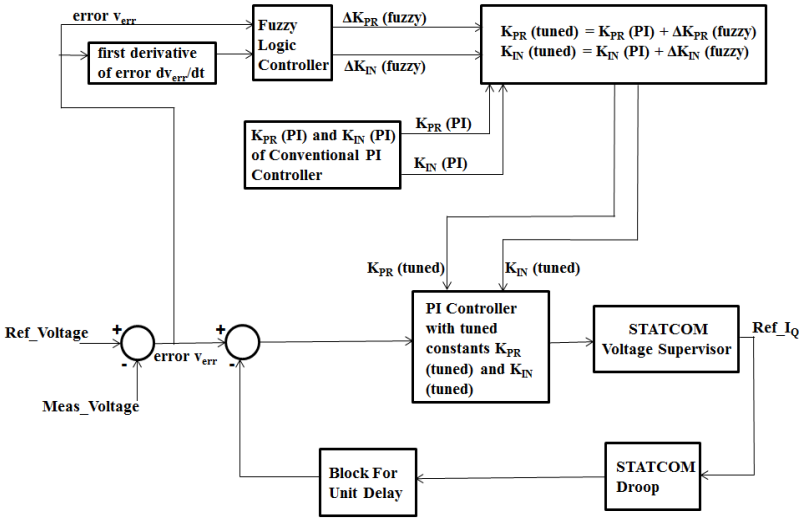

Figure 4. Block Schematic of STATCOM Voltage Supervisor Regulated Using Fuzzy-PI Technique

In the fuzzy-PI regulated STATCOM current supervisor, the difference between the reference reactive current (Ref_I_Q) and the measured (actual) value of reactive current ($Meas\_I_Q$), which is represented by i_{err}, and the first derivative of this deviation di_{err}/dt were fed as inputs to the fuzzy system. The fuzzy controller provided the required changes in controller gains, ΔK_{PR} (fuzzy) and ΔK_{IN} (fuzzy). The new PI controller with modified proportional and integral gain constants, K_{PR} (tuned) and K_{IN} (tuned), was used to control the STATCOM current supervisor. The angular shift between the AC bus voltage and the voltage of the converter, alpha, was provided by the STATCOM current regulator.

The rules applied to obtain ΔK_{PR} (fuzzy) and ΔK_{IN} (fuzzy) in the fuzzy systems in both the voltage and current supervisors are presented in Table 1 and Table 2 respectively. In the membership functions and rule tables, nvb, nb, z, pb and pvb stand for "negative very big", "negative big", "zero", "positive big" and "positive very big" respectively. If error and its first derivative are of greater magnitudes, ΔK_{PR} is also greater. By making ΔK_{IN} zero in case of very large magnitudes of error and its derivative, control saturation can be avoided. Steady state error can be certainly diminished if the values of ΔK_{IN} corresponding to small values of error are large [14].

Table 1. Fuzzy Rule Base for ΔK_{PR}: Voltage and Current Supervisors in STATCOM Controller

dv_{err}/dt or di_{err}/dt ↓ \ v_{err} or i_{err} →	NVB	NB	Z	PB	PVB
NVB	nb	nb	nb	pb	z
NB	nb	nb	z	z	pb
Z	nb	nb	z	pb	pb
PB	nb	nb	z	pb	pb
PVB	z	nb	pb	pb	pb

Table 2. Fuzzy Rule Base for ΔK_{IN}: Voltage and Current Supervisors in STATCOM Controller

dv_{err}/dt or di_{err}/dt ↓ \ v_{err} or i_{err} →	NVB	NB	Z	PB	PVB
NVB	z	nb	nb	nb	z
NB	z	nb	nb	z	z
Z	z	z	z	pb	z
PB	z	z	pb	pb	z
PVB	z	pb	pb	pb	z

The difference between the grid (reference) frequency and the frequency of the DFIG, f_{err}, and its first derivative, df_{err}/dt, were provided as inputs to the STATCOM frequency regulator. The change in STATCOM reference reactive current, ΔRef_I_Q, was provided as output by the fuzzy supervised frequency regulator. This change in STATCOM reference reactive current, ΔRef_I_Q, was added to Ref_I_Q provided by the voltage regulator to obtain the final value of the STATCOM reference reactive current.

The rules applied to obtain ΔRef_I_Qin the fuzzy system in the frequency controller are displayed in Table 3. Large magnitudes of fast rising frequency deviation demand a greater amount of STATCOM capacitive current since the electrical output of the alternators falls below the mechanical input supplied to them. In such situations, the transient stability of the line improves when the STATCOM supplies a greater magnitude of capacitive current since more power is transferred to the receiving end. It was therefore inferred that the STATCOM current must be positive large (mode of operation must be capacitive) when f_{err} and df_{err}/dt are positive large [15].

Table 3. Fuzzy Rule Base for Ref_I_Q: Frequency Regulator in STATCOM Controller

df_{err}/dt ↓ \ f_{err} →	NVB	NB	Z	PB	PVB
NVB	nvb	nb	nb	nb	nb
NB	nb	nb	nb	nb	nb
Z	nb	nb	z	pb	pb
PB	pb	pb	pb	pb	pb
PVB	pb	pb	pb	pb	pvb

5. RESEARCH METHOD 2: STATCOM CONTROLLED BY PSO

PSO was harnessed to adjust the PI controller gains in the STATCOM voltage supervisor, therefore this control methodology was termed PSO-PI technique. The optimized PI controller gains provided by the PSO program, K_{PR} (opt) and K_{IN} (opt), were used in the PSO-PI controlled STATCOM voltage supervisor, as shown in Figure 5. As stated earlier, the voltage regulator provides the STATCOM reference reactive current Ref_I_Q as its output, and the slope of the STATCOM V-I characteristics (in voltage control mode) is referred to as droop.All the steps in the flowchart for PSO for STATCOM control shown in Figure 6.

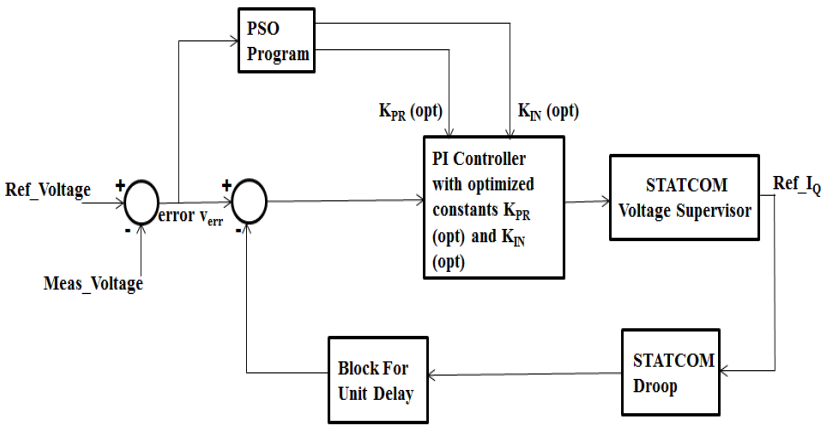

Figure 5. Block Schematic of STATCOM Voltage Supervisor Regulated Using PSO-PI Technique

Step 1: Initial conditions: In the PSO algorithm for STATCOM control, the gains of the PI controller K_{PR} and K_{IN} were the positions or searching points. The increments in controller gains ΔK_{PR} and ΔK_{IN} were the velocities. The specified ranges for K_{PR} and K_{IN} were chosen to be [0 1.5] and [0 1] respectively. The initial values of ΔK_{PR} and ΔK_{IN} were randomly chosen within the interval [-1 1]. Pbest (personal best) was the present position for each particle and gbest (global best) was the position of the particle with the best calculated value of evaluation function out of all available pbests.

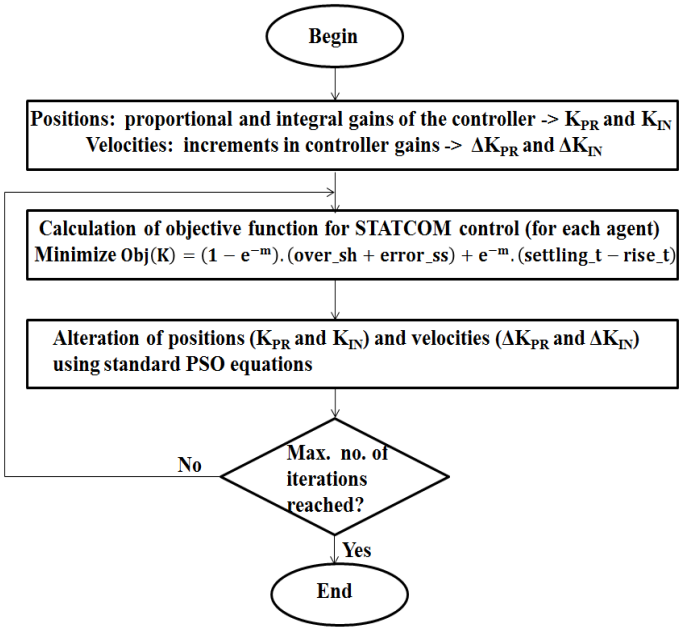

Figure 6. Flowchart for PSO for STATCOM supervision

Step 2: Attainment of evaluation function value for each agent: Some of the performance criteria commonly utilized for tuning PI controllers are integral absolute error (IAE), integral of squared error (ISE) and integral of time weighted squared error (ITSE). They have their own disadvantages. IAE and ISE can lead to a long settling time although they minimize the overshoot. In spite of the fact that ITSE overcomes the long settling time problem, it involves very complicated and lengthy analytical calculations. In this work, a different evaluation criterion was used. The objective functionObj (K), whose value was to be minimized in this case, is stated in Equation (12):

$$\mathrm{Obj(K)} = (1 - e^{-m}).(\mathrm{over\_sh} + \mathrm{error\_ss}) + e^{-m}.(\mathrm{settling\_t} - \mathrm{rise\_t}) \quad (12)$$

In Equation (12), K= [K_{PR} K_{IN}], error_ssstands for the error at steady-state, settling_t and rise_tstand for the settling time and rise time respectively, and the peak overshoot is denoted byover_sh. If the weighting factor m exceeds 0.7, the error at steady state and peak overshoot are decreased, and if it is below 0.7, the settling time and rise time are reduced [16]. Therefore, the preferred range for mis [0.8 1.5], in this program, m was taken to be 1.2. The performance criterion was evaluated for each agent. If a new searching point provided a better evaluated value of objective function, it replaced the current pbest. The best out of all available new pbests replaced the current gbest if it satisfied the design criterion in a better way compared to the present gbest.

Step 3: Updating positions and velocities: The controller gains and their increments were altered using the Equations (13), (14) and (15):

$$K_t^{j+1} = K_t^j + V_t^{j+1} = K_t^j + \Delta K_t^{j+1} \quad (13)$$

$$\Delta K_t^{j+1} = \mathrm{ind\_cnst} \times \mathrm{rdm\_1} \times \left(K_{t(\mathrm{pbest})} - K_t^j\right) + \mathrm{scl\_cnst} \times \mathrm{rdm\_2} \times \left(K_{\mathrm{gbest}} - K_t^j\right) + wf^j \, \Delta K_c^j \quad (14)$$

$$wf^j = w_{mx} - (w_{mx} - w_{mn})/\mathrm{iteration\_max}) \times j \quad (15)$$

In Equations (13), (14) and (15), K_t^j denotes the position of the particle t at iteration j, K_t^{j+1} stands for the location of particle t at iteration j+1, $V_t^{j+1} = \Delta K_t^{j+1}$ is the velocity (increment in controller gain for t^{th} particle ΔK_t) of particle t at iteration j+1, ind_cnstand scl_cnstdenote the constants which account for individual and social behavior respectively, iteration_maxis the pre-specified maximum number of iterations, w_{mx} and w_{mn} denote the maximum and minimum inertia weights respectively, j is the number of the present iteration and rdm_1 and rdm_2 are random number sequences within the range [0 1].

Step 4: Check on exit condition: The exit condition was fulfilled if the current iteration count became equal to the maximum number of iterations, which was specified to be 24 in this case.The parameters used in the PSO program for the STATCOM are summarized in Table 4.

Table 4. Parameters in the PSO program for STATCOM control

Parameter	Value
Number of Particles	10
Constant for Individual Representation (ind_cnst)	2
Constant Representing Social Interactions (scl_cnst)	2
Maximum (Initial) Inertia Weight (w_{mx})	1.5
Minimum (Final) Inertia Weight (w_{mn})	0.5
Total number of iterations considered (iteration_max)	24
Weighting Factor (m)	1.2

6. RESEARCH METHOD 3: STATCOM CONTROLLED BY FUZZY LOGIC AND PSO

In the fourth methodology, the proportional and integral PI gains of the STATCOM voltage supervisor weretuned using both fuzzy logic and PSO (combination of fuzzy-PI and PSO-PI techniques), hence this technique was called fuzzy PSO-PI technique. The schematic diagram of the STATCOM voltage regulator supervised using fuzzy PSO-PI technique is shown in Figure 7. K_{PR} (PSO) and K_{IN} (PSO) obtained from the PSO program described in section 5were added to ΔK_{PR} (fuzzy) and ΔK_{IN} (fuzzy) obtained from the fuzzy controller described in section 4, to get the final optimized tuned PI gains K_{PR} (final) and K_{IN} (final). As described in section 4, the current regulator was supervised using the fuzzy-PI technique and the frequency regulator was controlled using fuzzy logic.

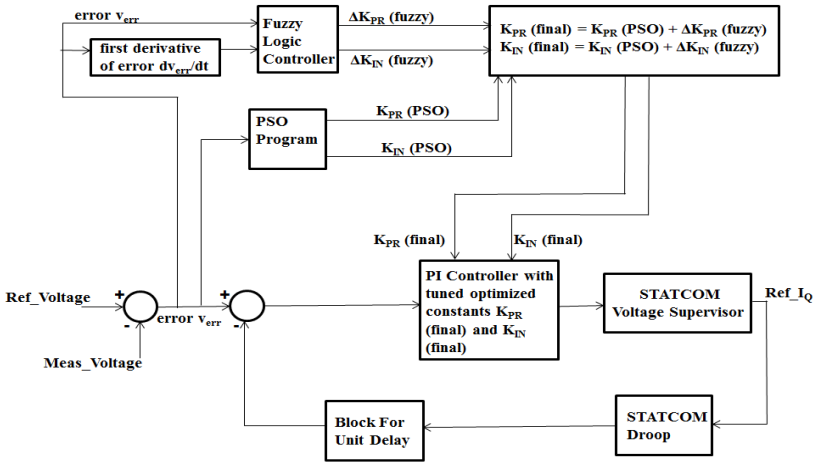

Figure 7. Block Schematic of STATCOM Voltage Supervisor Regulated Using Fuzzy PSO-PI Technique

7. TEST SYSTEM TOPOLOGY

The test system, whose single linediagram can be seen in Figure 8, was simulated using SimPowerSystems, which is a component of MATLAB/SIMULINK and its parameters are specified in Table 5. The three loads in the test system named Load1, Load2 and Load3 are a 355 MW resistive load, a 450 MW resistive load and a 550 KW, 100 KVAR R-L load respectively. The voltage compensation provided by the 48-pulse GTO based STATCOM at the PCC (bus named 'BUS_PCC') is validated in five test cases. In test case one, the speed of the wind was set to drop suddenly at time t=0.1 seconds from 22 m/s to 3 m/s. This was accompanied by a dip in the voltage of the grid to 0.1 pu, which was however brought back to its normal

value of 1 pu at time t=0.14 seconds. In test cases two, three and four, the voltage dip was observed at the bus labeled 'BUS_PCC' as a consequence of SLG, LL and DLG faults respectively at time t=0.1 seconds for two cycles at the terminals of the bus labelled 'BUS_FAULT'. The fifth and last test case dealt with an abrupt rise in load at the bus named BUS_PCC. Prior to the load change, the total resistive load at BUS_PCC was 500 KW. By gating an extra 500 MW resistive load at time t=0.1 seconds at BUS_PCC, the resultant resistive load at BUS_PCC became (500 KW + 500 MW), which implied an increment in load at BUS_PCC by a little more than a thousand times. The additional 500 MW load was switched off after two cycles. The speed of the wind was maintained at 15 m/s in all the cases except the first one. The total simulation time was 0.2 seconds in all the test cases. For all the five test cases, the test system was simulated four times, first without the STATCOM, second with fuzzy controlled STATCOM, third with PSO controlled STATCOM, and fourth, with fuzzy PSO controlled STATCOM. Using all the three control techniques separately in the five testcases, the positive sequence voltage was observed at the bus named 'BUS_PCC', which was the point of common coupling (PCC).

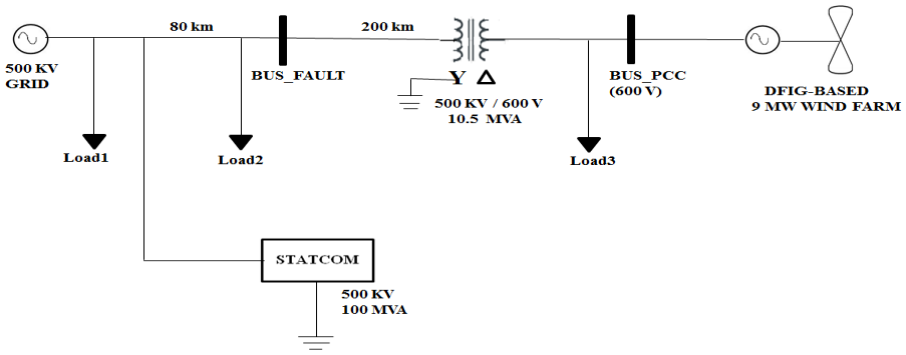

Figure 8. Test System Schematic

Table 5. Parameters of the DFIG-based wind farm, transmission line and STATCOM and its controller

DFIG-Based Wind Farm				STATCOM and Its Controller	
Parameter	Value	Parameter	Value	Parameter	Value
Total rated active power	1.5x6 = 9 MW	DFIG stator equivalent resistance	0.023 pu	Rated voltage	500 kV
Rated DC bus voltage (wind farm)	1150 V	DFIG stator equivalent inductance	0.18 pu	Rated apparent power	100 MVA
DC bus capacitance (wind farm)	10000μF	DFIG rotor equivalent resistance	0.016 pu	DC voltage source	two 3000 μF capacitors connected in series
Terminal voltage	600 V	DFIG frequency	60 Hz	Droop	0.03 pu / 100 MVA
Transmission Line (Distributed Parameters)				Voltage Regulator Gains	K_{PR}(PI) = 10 K_{IN}(PI) = 2
Positive sequence resistance/unit length	0.0255 ohm/km	Positive sequence capacitance/unit length	12.74e-9 F/km	Current Regulator Gains	K_{PR}(PI) = 5 K_{IN}(PI) = 40
Positive sequence inductance/unit length	0.9337e-3 H/km			Sample Time	2.5e-5 seconds

8. RESULTS AND ANALYSIS

The voltage magnitudes at BUS_PCC for all the test cases using STATCOM controlled by all the three artificial intelligence based techniques are listed in Table 6.

Three important points can be derived from the results tabulated in Table 6:

a. Improvement in the positive sequence voltage at BUS_PCC (common coupling point) is observed in all the test cases, using STATCOM controlled by all the three techniques, namely, fuzzy logic, PSO and fuzzy-PSO. Therefore, in such situations, owing to the dynamic voltage support provided by the

STATCOM, it is not required to detach the DFIG-based wind farm from the main grid-connected system during voltage dips. Thus, the grid codes related to stable operation of wind farms in case of voltage sags are not violated.

b. It is noted that for the first two cases, namely, simultaneous drop in wind speed and grid voltage and SLG fault, the STATCOM controlled using PSO provided the maximum voltage compensation out of the three techniques.

c. It is seen that in the remaining test cases, namely, LL fault, DLG fault and sudden load increment, the fuzzy PSO controlled STATCOM offered the highest improvement in voltage at the PCC.

The detailed simulation results and associated analysis for all the test cases in the form of a performance comparison among the three STATCOM control techniques described in sections 4, 5 and 6 are presented.

Table 6. Positive sequence voltage at BUS_PCC in all the test cases using STATCOM controlled by all the three techniques

Type of disturbance	Positive sequence voltage (pu) at BUS_PCC when STATCOM is absent	Positive sequence voltage (pu) at BUS_PCC when fuzzy controlled STATCOM is present	Positive sequence voltage (pu) at BUS_PCCwhen PSO controlled STATCOM is present	Positive sequence voltage (pu) at BUS_PCC when fuzzyPSO controlled STATCOM is present
Simultaneous occurrence of step change (drop) in wind speed and voltage dip on grid	0.68	0.92	0.95	0.94
Single line to ground fault	0.75	0.98	0.995	0.99
Line to line fault	0.55	0.78	0.79	0.8
Double line to ground fault	0.4	0.575	0.586	0.591
Sudden increment in load	0.69	0.89	0.86	0.897

8.1. Simultaneous Occurrence of Step Change (Drop) in Wind Speed and Dip in the Grid Voltage

When the wind speed dropped as a step from 22 m/s to 3 m/s and the grid voltage dipped to 0.1 pu simultaneously, the positive sequence voltage at BUS_PCC, which had fallen to 0.68 pu in the absence of STATCOM (Figure 9) improved to 0.92 pu, 0.95 pu and 0.94 pu in the presence of fuzzy, PSO (Figure 10) and fuzzy PSO controlled STATCOM respectively. Therefore, we see that the STATCOM controlled using PSO provided the highest voltage compensation out of the three methods. It can also be observed from Figure 11 that the fuzzy PSO controlled STATCOM offered a comparatively smoother voltage response, with fewer oscillations.

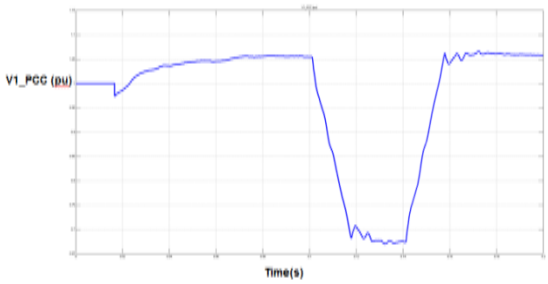

Figure 9. Positive sequence voltage (pu) at BUS_PCC under the impact of step change (drop) in wind speed and voltage dip on the grid when STATCOM is absent

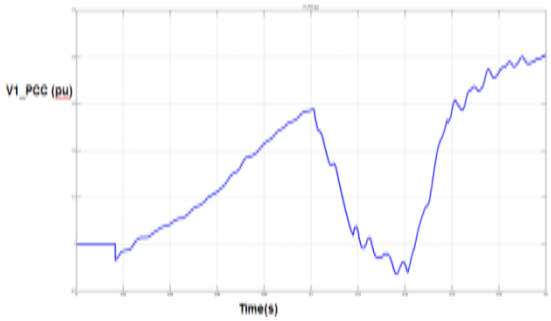

Figure 10. Positive sequence voltage (pu) at BUS_PCC under the impact of step change (drop) in wind speed and voltage dip on the grid when PSO controlled STATCOM is included in the system

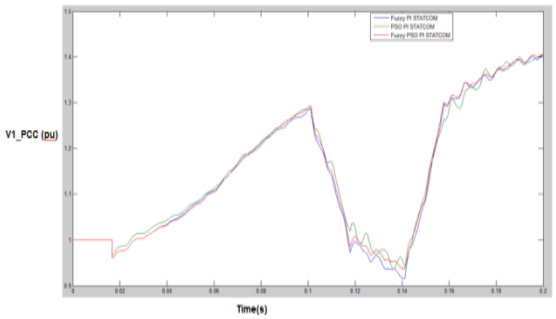

Figure 11. Positive sequence voltage (pu) at BUS_PCC for simultaneous occurrence of step change (drop) in wind speed and grid voltage dip: fuzzy (blue), PSO (green) and fuzzy PSO (red) controlled STATCOM

8.2. Single Line to Ground Fault

It can be seen in figures 12-14 that the positive sequence voltage at BUS_PCC which had dipped to 0.75 pu as a consequence of SLG fault at BUS_FAULT, improved to 0.98 pu when fuzzy controlled STATCOM was connected, 0.995 pu when PSO controlled STATCOM was connected and 0.99 pu when fuzzy PSO controlled STATCOM was connected. Thus, in this case, the PSO controlled STATCOM provided slightly more improvement in voltage compared to STATCOM controlled by the other techniques, as seen in Figure 14.

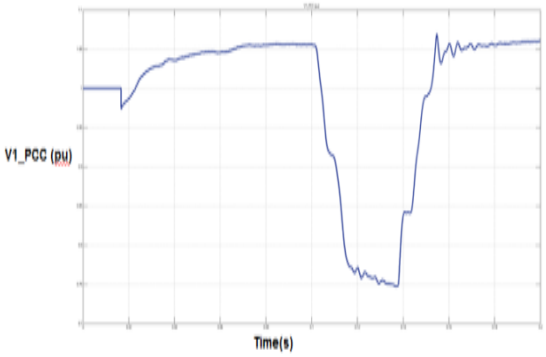

Figure 12. Positive sequence voltage (pu) at BUS_PCC when an SLG fault occured at BUS_FAULT and STATCOM is not present in the system

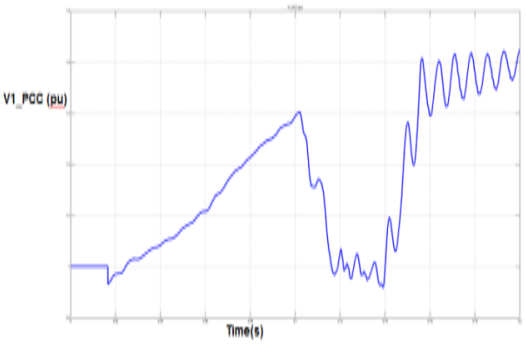

Figure 13. Positive sequence voltage (pu) at BUS_PCC when an SLG fault occured at BUS_FAULTand PSO controlled STATCOM is present in the system

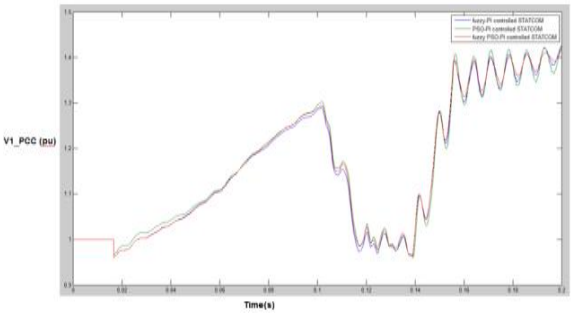

Figure 14. Positive sequence voltage (pu) at BUS_PCC for SLG fault: fuzzy (blue), PSO (green) and fuzzy PSO (red) controlled STATCOM

8.3. Line To Line Fault

As a result of LL fault at BUS_FAULT, the positive sequence voltage at BUS_PCC, which had dropped to 0.55 pu in the absence of STATCOM (Figure 15), improved to 0.78 pu, 0.79 pu and 0.8 pu in the presence of fuzzy, PSO and fuzzy PSO (Figure 16) controlled STATCOM respectively. Therefore, it was observed that the fuzzy-PSO controlled STATCOM offered the highest voltage improvement out of all the three techniques, as seen in Figure 17. It is also clear from Figure 17 that the fuzzy-PSO controlled STATCOM offered a comparatively more stable voltage response with reduced magnitude and frequency of oscillations.

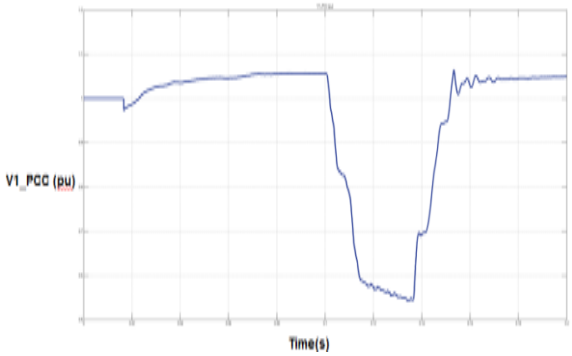

Figure 15. Positive sequence voltage (pu) at BUS_PCC when an LL faultoccured at BUS_FAULT and STATCOM is not present in the system

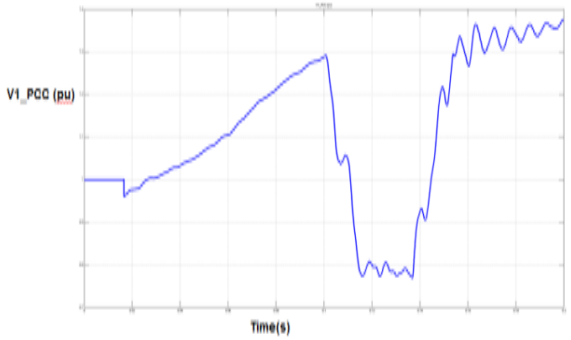

Figure 16. Positive sequence voltage (pu) at BUS_PCC when an LL fault occured at BUS_FAULT and fuzzy PSO controlled STATCOM is present in the system

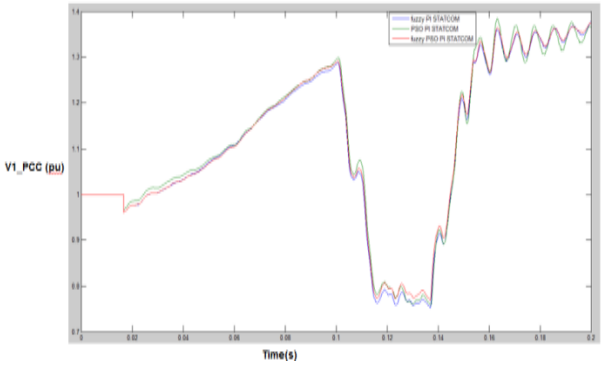

Figure 17.Positive sequence voltage (pu) at BUS_PCC for LL fault: fuzzy (blue), PSO (green) and fuzzy PSO (red) controlled STATCOM

8.4. Double Line to Ground Fault

Due to DLG fault at BUS_FAULT, the positive sequence voltage at BUS_PCC, which had sagged to 0.4 pu when STATCOM was not present (Figure 18), rose to 0.575 pu, 0.586 pu and 0.591 pu when STATCOM controlled by fuzzy, PSO and fuzzy PSO techniques (Figure 19) respectively, was incorporated in the system. The voltage magnitude improved to the maximum extent and the response became comparatively smoother when fuzzy- PSO controlled STATCOM was employed (seen in Figure 20).

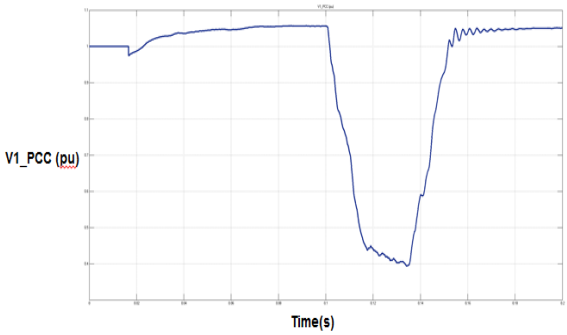

Figure 18. Positive sequence voltage (pu) at BUS_PCC when a DLG fault occured at BUS_FAULT and STATCOM is not present in the system

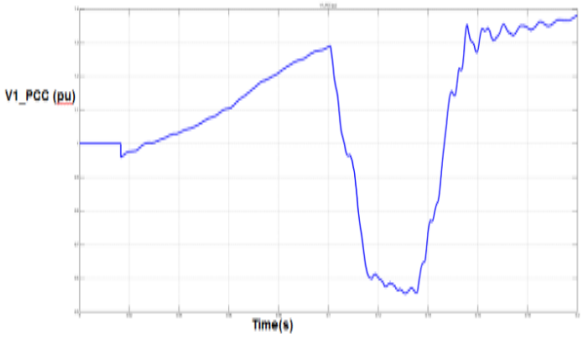

Figure 19. Positive sequence voltage (pu) at BUS_PCC when a DLG fault occured at BUS_FAULT and fuzzy PSO controlled STATCOM is present in the system

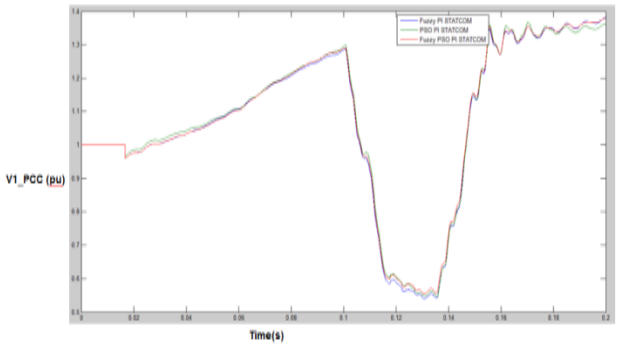

Figure 20. Positive sequence voltage (pu) at BUS_PCC for DLG fault: fuzzy (blue), PSO (green) and fuzzy PSO (red) controlled STATCOM

8.5. Sudden Increment in Load by More Than Thousand Times

Corresponding to a sudden increment in load by more than a thousand times as described in section 7, the voltage at BUS_PCC, which had decreased to 0.69 pu in the absence of STATCOM (Figure 21), increases to 0.89 pu when fuzzy controlled STATCOM was connected, and increased to 0.897 pu, when fuzzy-PSO controlled STATCOM was incorporated (can be seen in Figure 22).

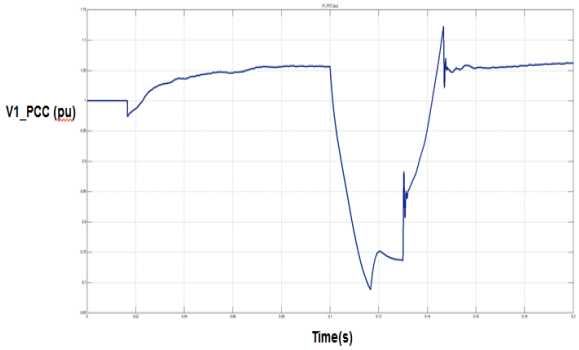

Figure 21. Positive sequence voltage (pu) at BUS_PCC under the impact of a sudden increment in load at the PCC when STATCOM is not present in the system

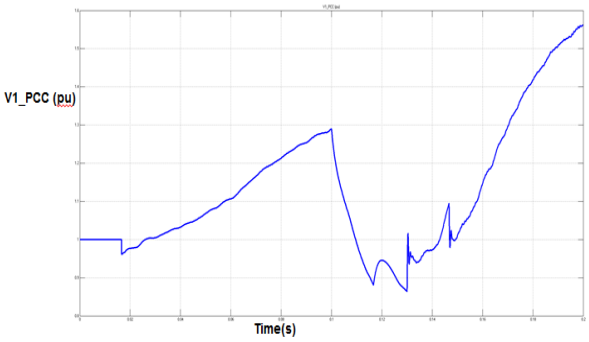

Figure 22. Positive sequence voltage (pu) at BUS_PCC under the impact of a sudden increment in load at the PCC when fuzzy PSO controlled STATCOM is present in the system

9. CONCLUSION

The STATCOM controlled by the three soft computing techniques, namely, fuzzy logic, PSO and a combination of both was able to provide voltage compensation at the PCC in all the test cases.It was observed that the PSO controlled STATCOM offered the highest voltage improvement in the first two cases, step change (drop) in wind speed simultaneously accompanied by grid voltage dip and SLG fault. In cases of LL fault, DLG fault and sudden rise in load, the STATCOM controlled by fuzzy-PSO technique provided the maximum voltage compensation. Additionally, in all the test cases, it was noted that the voltage response at the PCC provided by the STATCOM controlled by fuzzy-PSO technique was relatively smoother, with few oscillations.Thus, under such circumstances, with the help of the STATCOM, voltage instability due to severe voltage sags is prevented, hence the need for disconnecting the wind turbines due to voltage drops does not arise, and therefore, grid codes (related to low voltage ride-through) are satisfied.In future, the latest variants of PSO and recent hydrid artificial intelligence based techniques may be used to control the STATCOM which provides voltage compensation.

REFERENCES

[1] Hemant Ahuja, G. Bhuvaneswari and R. Balasubramanian *"Performance Comparison of DFIG and PMSG Based WECS"*, IET Conference on Renewable Power Generation, 2011.

[2] R. Arindya, "A Variable Speed Wind Generation System Based on Doubly Fed Induction Generator", *Bulletin of Electrical Engineering and Informatics*, Vol. 2, No. 4, pp. 272-277, December 2013.

[3] Sharad W. Mohod and Mohan V. Aware, "A STATCOM-Control Scheme for Grid Connected Wind Energy System for Power Quality Improvement", *IEEE Systems Journal*, vol. 4, no.3, September 2010.

[4] Wei Qiao, Ganesh Kumar Venayagamoorthy and Ronald G. Harley, "Real-time implementation of a STATCOM on a wind farm equipped with doubly fed induction generators", *IEEE Transactions on Industry Applications*, vol. 45, no. 1, pp. 98–107, Feb. 2009.

[5] Wei Qiao, Ganesh Kumar Venayagamoorthy, and Ronald G. Harley, "Coordinated reactive power control of large wind farm and a STATCOM using heuristic dynamic programming", *IEEE Transactions on Energy Conversion*, vol. 24, no. 2, pp. 493–503, June 2009.

[6] Bhupendra Sehgal, S.P. Bihari, YogitaKumari, R.N. Chaubey and Anmol Gupta, "Performance of FACTS Devices for Power System Stability", *Indonesian Journal of Electrical Engineering and Informatics (IJEEI)*, Vol. 3, No. 3, pp. 135-140, September 2015.

[7] SA Gawish, SM Sharaf and MS El-Harony, "Voltage Stabilization of a Wind Turbine with STATCOM Using Intelligent Control Techniques", *Indonesian Journal of Electrical Engineering and Informatics (IJEEI)*, Vol. 4, No. 1, pp. 24-34, March 2016.

[8] An Luo, Ci Tang, Zhikang Shuai, Jie Tang, Xian Yong Xu and Dong Chen, "Fuzzy-PI-Based Direct-Output-Voltage Control Strategy for the STATCOM Used in Utility Distribution Systems", published in *IEEE Transactions on Industrial Electronics*, Vol. 56, No. 7, July 2009.

[9] Chien-Hung Liu and Yuan-Yih Hsu "Design of a Self-Tuning PI Controller for a STATCOM Using Particle Swarm Optimization", published in *IEEE Transactions on Industrial Electronics*, Vol. 57, No. 2, February 2010.

[10] Alfred Wanyama Manyonge, Reccab Manyala, F.N. Onyango and J. Shichika, "Mathematical modelling of wind turbine in a wind energy conversion system: Power coefficient analysis", *Applied Mathematical Sciences*, Vol. 6, no. 91, 4527 – 4536, 2012.

[11] A. Babaie Lajimi, S. Asghar Gholamian and M. Shahabi, "Modeling and Control of a DFIG-Based Wind Turbine During a Grid Voltage Drop", published in *Engineering, Technology and Applied Science Research*, Vol. 1, No. 5, 121-125, 2011.

[12] Keyou Wang, "Power System Voltage Regulation via STATCOM Internal Nonlinear Control", *IEEE Transactions on Power Systems*, 26(3), pp-1252-1262, August 2011.

[13] Narain G. Hingorani and Laszlo Gyugyi "Understanding FACTS, Concepts and Technology of Flexible AC Transmission Systems", IEEE Press, 2000.

[14] Surinder Chauhan, Vikram Chopra and Shakti Singh, *"Power System Transient Stability Improvement using Fuzzy PI Based STATCOM Controller"*, published in 2nd International Conference on Power, Control and Embedded Systems, 2012.

[15] A. Ghafouri, M.R. Zolghadri, M. Ehsan, O. Elmatboly and A. Homaifar, *"Fuzzy Controlled STATCOM for Improving Power System Transient Stability*," published in IEEE Conference Publications, Power Symposium, NAPS 2007.

[16] Zwe-Lee Gaing, "A Particle Swarm Optimization Approach for Optimum Design of PID Controller in AVR System", published in *IEEE Transactions on Energy Conversion*, Vol. 19. No. 2, June 2004.